Draft version December 9, 2011
Preprint typeset using LaTeX style emulateapj v. 08/13/06

DWARFS GOBBLING DWARFS: A STELLAR TIDAL STREAM AROUND NGC 4449 AND HIERARCHICAL GALAXY FORMATION ON SMALL SCALES

David Martínez-Delgado[1,13], Aaron J. Romanowsky[2], R. Jay Gabany[3], Francesca Annibali[4], Jacob A. Arnold[2], Jürgen Fliri[5,6], Stefano Zibetti[7], Roeland P. van der Marel[8], Hans-Walter Rix[1], Taylor S. Chonis[9], Julio A. Carballo-Bello[10], Alessandra Aloisi[8], Andrea V. Macciò[1], J. Gallego-Laborda[11], Jean P. Brodie[2], Michael R. Merrifield[12]

(Received; Accepted)
Draft version December 9, 2011

ABSTRACT

We map and analyze a stellar stream in the halo of the nearby dwarf starburst galaxy NGC 4449, detecting it in deep integrated-light images using the Black Bird Observatory 0.5-meter telescope, and resolving it into red giant branch stars using Subaru/Suprime-Cam. The properties of the stream imply a massive dwarf spheroidal progenitor, which will continue to disrupt and deposit an amount of stellar mass that is comparable to the existing stellar halo of the main galaxy. The ratio between luminosity or stellar-mass between the two galaxies is $\sim$ 1:50, while the dynamical mass-ratio when including dark matter may be $\sim$ 1:10–1:5. This system may thus represent a "stealth" merger, where an infalling satellite galaxy is nearly undetectable by conventional means, yet has a substantial dynamical influence on its host galaxy. This singular discovery also suggests that satellite accretion can play a significant role in building up the stellar halos of low-mass galaxies, and possibly in triggering their starbursts.

Subject headings:

1. INTRODUCTION

A fundamental characteristic of the modern cold dark matter (ΛCDM) cosmological paradigm (Mo et al. 2010) is that galaxies undergo hierarchical assembly under the influence of gravity, continually accreting smaller DM halos up until the present day. If those halos contain stars, then they will be visible as satellites around their host galaxies, eventually disrupting through tidal forces into distinct streams and shells before phase-mixing into obscurity (Cooper et al. 2010). This picture seems to explain the existence of satellites and substructures around massive galaxies in the nearby Universe (Arp 1966; Schweizer & Seitzer 1988; McConnachie et al. 2009; Martínez-Delgado et al. 2010). However, a quantitative confirmation of this aspect of ΛCDM has been more elusive, while there are some lingering doubts about the consonance with ΛCDM of small-scale substructure observations (Lovell et al. 2011; Boylan-Kolchin et al. 2011; Ferrero et al. 2011).

To date there has been relatively little work on substructure and merging in the halos around low-mass, "dwarf" galaxies. Many cases of extended stellar halos around dwarfs have been identified observationally (see review in Stinson et al. 2009), but it is not clear if these stars were accreted, or formed in situ. Star formation in dwarf galaxies is thought to occur in stochastic episodes (Tolstoy et al. 2009; Weisz et al. 2011), which could in principle be triggered by accretion events.

An iconic galaxy in this context is NGC 4449, a dwarf irregular in the field that has been studied intensively as one of the strongest galaxy-wide starbursts in the nearby Universe. Its absolute magnitude of $M_V = -18.6$ makes it an LMC-analogue (and not formally a dwarf by some definitions), except that its star formation rate is $\sim$ 10 times higher. It is strongly suspected to have recently interacted with another galaxy based on various signatures including peculiar kinematics in its cold gas and HII regions (Hartmann et al. 1986; Hunter et al. 1998), but the nature of this interaction is unknown.

An elongated dwarf galaxy or stream candidate near NGC 4449 was first noticed by Karachentsev et al. (2007) based on Digitized Sky Survey (POSS-II) plates (object d1228+4358), which is also visible in archival images from the Sloan Digital Sky Survey (SDSS; Abazajian et al. 2009). Here we present deep, wide-field optical imaging that supplies the definitive detection of this ongoing accretion event involving a smaller galaxy, leading to interesting implications about the evolution of this system and of dwarf galaxies in general.

2. OBSERVATIONS AND DATA REDUCTION

Our observations of NGC 4449 and its surroundings consist of two main components. The first is imaging from a small robotic telescope to confirm the presence

[1] Max-Planck-Institut fur Astronomy, Heidelberg, Germany
[2] University of California Observatories, Santa Cruz, CA 95064, USA
[3] Black Bird Observatory, Mayhill, New Mexico, USA
[4] Osservatorio Astronomico di Bologna, INAF, Via Ranzani 1, I-40127 Bologna, Italy
[5] LERMA, CNRS UMR 8112, Observatoire de Paris, 61 Avenue de l'Observatoire, 75014 Paris, France
[6] GEPI, CNRS UMR 8111, Observatoire de Paris, 5 Place Jules Janssen, 92195 Meudon, France
[7] Dark Cosmology Centre, Niels Bohr Institute - University of Copenhagen, Juliane Maries Vej 30, DK-2100 Copenhagen, Denmark
[8] Space Telescope Science Institute, 3700 San Martin Drive, Baltimore, MD 21218
[9] Department of Astronomy, University of Texas at Austin, Texas, USA
[10] Instituto de Astrofisica de Canarias, Tenerife, Spain
[11] Fosca Nit Observatory, Montsec Astronomical Park, Ager, Spain
[12] School of Physics and Astronomy, University of Nottingham, University Park, Nottingham NG7 2RD, England
[13] Alexander von Humboldt Fellow for Advanced Research

of a low-surface-brightness substructure in the halo of NGC 4449 and to provide its basic characteristics (similar techniques were used to study substructures around larger galaxies in Martínez-Delgado et al. 2008, 2010). The second is follow-up imaging with the Subaru telescope to map out the resolved stellar populations.

First, we obtained very deep images with the f/8.3 Ritchey-Chretien 0.5-meter telescope of the Black Bird Remote Observatory (BBRO)[14] during different dark-sky observing runs during the periods 2010-04-13 through 2010-06-10, and 2011-01-13 through 2011-01-28 (UT). We used a 16 mega-pixel Apogee Imaging Systems U16M CCD camera, with $31.3' \times 31.3'$ field-of-view and 0.46 arcsec pix^{-1} plate-scale. We acquired 18 hours of imaging data in half-hour sub-exposures, using a non-infrared clear luminance (λ = 3500–8500Å) Astrodon E-series filter. Each sub-exposure was reduced following standard procedures for dark-subtraction, bias-correction, and flat-fielding (see Martínez-Delgado et al. 2009).

The resulting image was calibrated photometrically to SDSS by comparing the brighter regions of NGC 4449 following the techniques of Martínez-Delgado et al. (2010). The final image has 5-σ g-band surface-brightness detection limits from 26.4 to 27.5 mag arcsec^{-2} for seeing-limited and large-scale diffuse features, respectively.

Second, we obtained images from the 8.2-m Subaru Telescope and the Suprime-Cam wide field imager ($34' \times 27'$ field-of-view and $0.202''$ pixel-scale; Miyazaki et al. 2002) on 2011-01-05 (UT). Conditions were photometric, and we took exposures in the r' and i' bands with a five-pointing dithering pattern. The total exposure times were 225 sec per filter. We reduced the data using our own modified version of the SDFRED pipeline (Ouchi et al. 2004), including scripts for bias subtraction, flat fielding, and distortion correction. Each frame was then re-projected to a common astrometric coordinate system followed by background rectification and image co-addition using the Montage toolkit[15].

The exquisite image quality ($\sim 0.5''$ FWHM) allows us to resolve individual stars in the outer regions of NGC 4449. We carried out stellar point-spread-function photometry using DAOPHOT II/ALLSTARS (Stetson 1987), and identified stars as objects with sharpness parameter $|S| < 1.0$. We then calibrated the photometry based on two central images from the *Hubble Space Telescope* Advanced Camera for Surveys (HST/ACS) (Annibali et al. 2008, hereafter A+08).

The ACS photometry was originally in F555W and F814W, and recalibrated to Johnson-Cousins VI (A+08). We used fairly bright, red stars in common between the datasets to derive linear transformation equations from $r'i'$ instrumental magnitudes to VI, including foreground extinction corrections of $E(B-V) = 0.019$ (Schlegel et al. 1998). Our final star catalog has statistical internal errors in $V-I$ color of ~0.11 mag and ~0.14 mag. at V=25 and V=26, respectively.

3. STREAM MORPHOLOGY

Figure 1 (*left*) shows a BBRO image subsection, where with an adopted distance of 3.82 Mpc (A+08), $1'$ corresponds to 1.1 kpc. Clearly visible near the minor axis of NGC 4449, ~ 10 kpc to the southeast, is a very elongated, S-shaped feature with a size of $\sim 1.5 \times 7$ kpc, which we will hereafter designate "the stream". The stream's position does not overlap with any of the complex HI-gas features surrounding NGC 4449 (Hunter et al. 1998). Also, it is on the opposite side of the galaxy with respect to an interesting star cluster that may be linked to another past accretion event (Annibali et al. 2011). The main galaxy's existing stellar halo can also be seen, including shell-like features in the southwest that were noticed by Hunter et al. (1999).

The right-hand panel shows a Suprime-Cam zoom-in of the stream. It is clearly resolved into stars and has the general appearance of a dwarf spheroidal (dSph) galaxy that is elongated by tides. This classification (defined by a spheroidal morphology, stellar mass $M_\star < 10^8 M_\odot$, and the absence of star formation and cold gas) is also supported by the HI non-detection of Huchtmeier et al. (2009).

To complement these integrated surface-brightness maps, we next construct stellar-density maps around NGC 4449 using individual RGB stars down to $g' = 25.8$ from Suprime-Cam. We will discuss the RGB selection and modeling later, but in general we can consider these stars as tracing a population older than 1 Gyr. We define a grid across the image with 130×130 pc^2 bins, and count the number of stars in each bin, subsequently applying a Gaussian smoothing kernel with $\sigma = 130$ pc. There are typically 7–9 stars per bin in the stream.

Figure 2(a) shows the resulting Subaru-based stellar density map, where the overall stream morphology is indistinguishable from the BBRO integrated-light results. Given that in the next Section we will find no evidence for resolved young stars, the simplest inference is that the visible light is dominated by RGB stars and hence by a population older than 1 Gyr.

Panel (b) shows a higher-contrast version of the same map, demonstrating that the main galaxy's pre-existing stellar halo extends out to at least ~ 10 kpc. We can furthermore discern a very faint feature that seems to extend the stream's angular path in a loop-like structure. This loop is also apparent in the BBRO image, and we infer that the stream is stretched out over at least half its orbit, with the projected turning point at a galactocentric radius of 13 kpc.

We next wish to locate the disrupting satellite galaxy's original center or nucleus. In both the BBRO and Subaru images there is a density enhancement near the mid-point of the "S", as would be expected if the "arms" are leading and trailing tidal tails around a still marginally-bound, or just disrupting, main body. We next construct a stellar-density contour map for the stream region, using the RGB stars and $\sigma = 270$ pc smoothing. The central stellar clump is visible in Figure 2(d), with a position slightly offset from the stream's main ridgeline $(\alpha(J2000), \delta(J2000)) = (12h\ 28m\ 43.320s, +43^\circ\ 58'\ 30.00'')$, The positional uncertainty is $\sim 6''$. An off-center nucleus is also seen in a tidally-disrupting Milky Way dSph, Ursa Major (Martínez-Delgado et al. 2001).

[14] BBRO was originally situated in the Sacramento Mountains (New Mexico, USA), and later moved to the Sierra Nevada Mountains (California, USA).

[15] http://montage.ipac.caltech.edu/

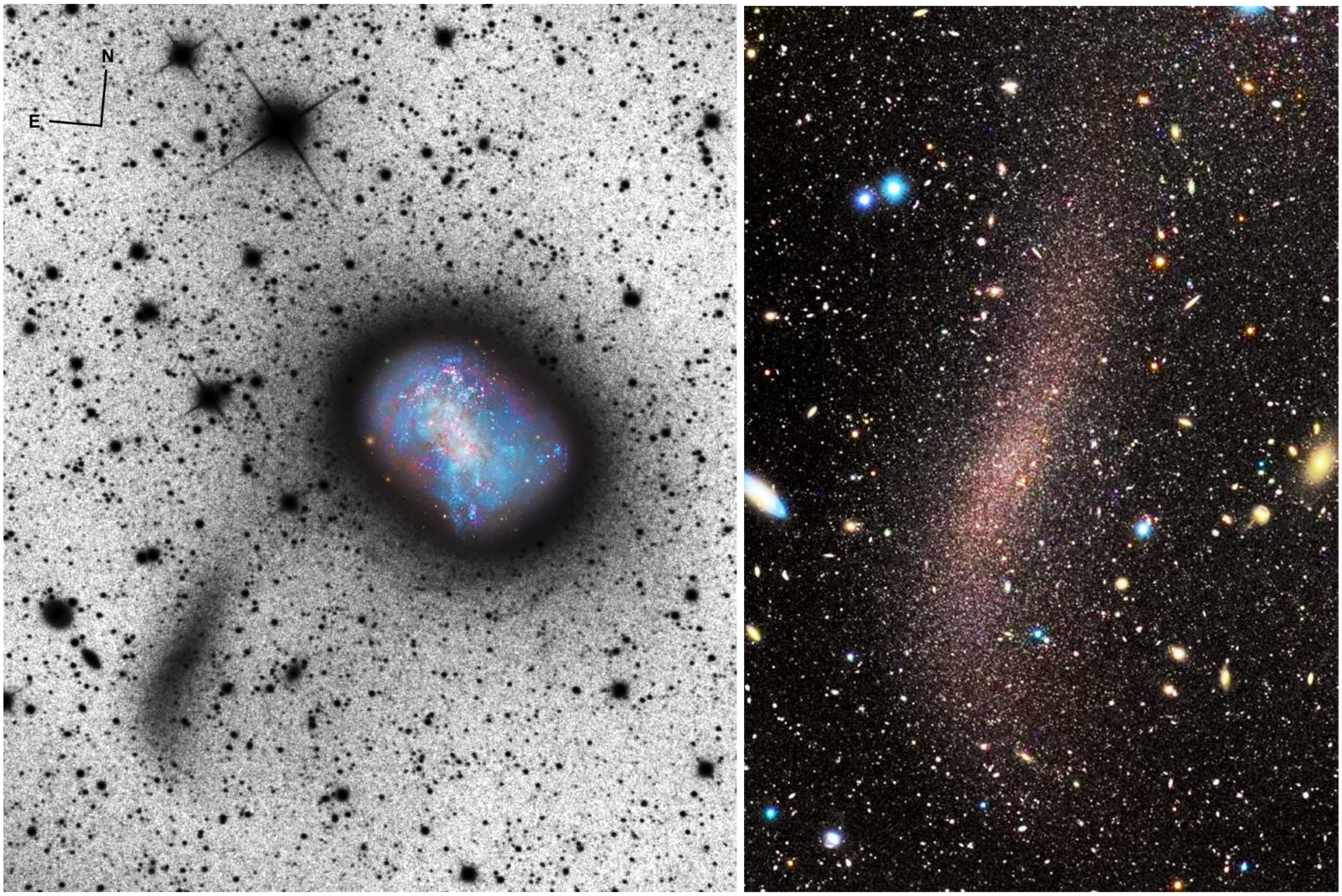

Fig. 1.— NGC 4449 and its halo stream. *Left:* image from the BBRO 0.5-m telescope, showing a 21×27 kpc field. *Right:* 6×9.5 kpc subsection of the Subaru/Suprime-Cam data, showing the stream resolved into stars. In both panels, shallower BBRO exposures in red/green/blue filters are used to provide indicative colors.

4. STELLAR POPULATIONS

Figure 3 shows the color-magnitude diagram (CMD) for point sources in the stream region. The RGB stars are the dominant feature, along with a few brighter, redder stars that may be oxygen- or carbon-rich thermally-pulsating asymptotic giant branch stars from an intermediate-age or old population (Marigo et al. 2003). There are no blue stars evident that would trace recent star formation.

The detection of the tip of the RGB (TRGB) permits a distance estimate for the stream. We use the same approach described in A+08 and Cioni et al. (2000), and find a TRGB magnitude of $I_{\rm TRGB} = 24.06 \pm 0.04$ (random) ± 0.08 (systematic). The random error was estimated using bootstrapping techniques; the systematic error is dominated by the magnitude transformation uncertainties. The main body of NGC 4449 was found by A+08 to have $I_{\rm TRGB} = 24.00 \pm 0.01$ (random) ± 0.04 (systematic). Thus the stream is at the same distance as the main body, to within ~ 180 kpc, and we conclude that there is a physical association rather than a chance superposition.

The RGB photometry can also constrain the stream age and metallicity, despite some age-metallicity degeneracy. In Figure 3 we overplot the Padua isochrones (Girardi et al. 2002) for ages of 2, 4, and 10 Gyr, for both $Z = 0.004$ and $Z = 0.001$. For $Z = 0.004$ the 2–4 Gyr isochrones trace the data reasonably well, while all $Z = 0.001$ models are too blue (by $\gtrsim 0.13$ mag: our systematic color uncertainties are $\lesssim 0.1$ mag). Presumably a 10 Gyr model with $Z \sim 0.002$ would also be consistent with the data, while perhaps providing a better match to the observed CMD slope. We thus find the stream to have an intermediate-to-old age ($\sim$ 2–10 Gyr) and a metallicity of $[Z/{\rm H}] \sim -0.9$ to -0.6.

These results are comparable to the RGB analysis of the main body of NGC 4449 by A+08 (their figure 17; see also Ryś et al. 2011). Therefore both the main galaxy and the stream contain similar old, intermediate-metallicity populations, although the main galaxy also contains very young stars, as well as more metal-poor stars as inferred from its globular clusters (Strader et al. 2011).

It is outside the scope of this Letter to investigate spatial stellar population variations in the stream and surrounding regions in detail, but we provide a basic overview by splitting the RGBs into color-based subpopulations, using the 4 Gyr, $Z = 0.004$ model as a boundary. We then create stellar density maps as before, for the two subpopulations separately. Using blue and green color-coding to represent the subpopulations left and right of the model boundary, we show the results in Figure 2(c). The stream's bright parts have no visible RGB color gradient, and have an overall color similar to the main galaxy's halo at radii of $\sim$ 3–5 kpc. Both the stream's faint-loop continuation, and the halo at $\sim$ 5–10 kpc, are redder, implying older or more metal-rich

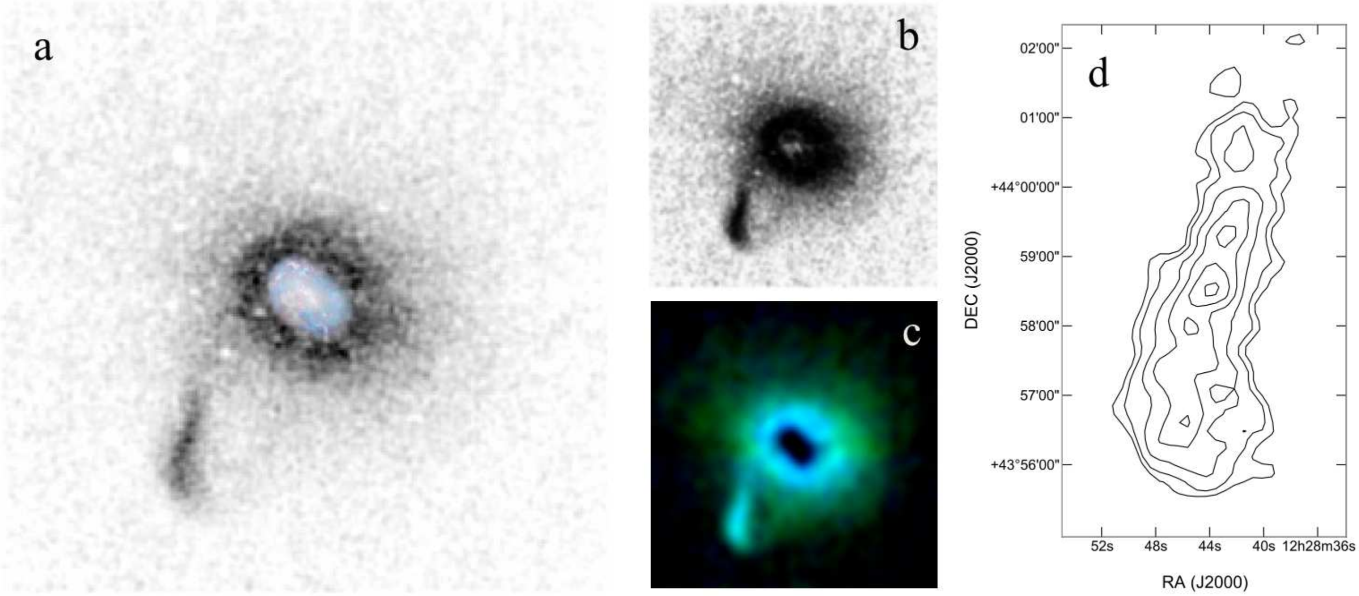

Fig. 2.— Stellar density maps of NGC4449 and its stream, based on RGB counts from Suprime-Cam. Panel (a) shows a 33 × 33 kpc image with linear scaling. There is a compact density enhancement within the stream, which may be the progenitor galaxy's remnant nucleus. Panel (b) shows the same data with less dynamic range. The stream shows a loop-like structure curving back toward the main galaxy, which in turn also shows a shell-like overdensity in its halo toward the southwest, reaching similar projected galactocentric radii as the stream. Panel (c) shows a composite map of the stream, color-coded blue for bluer RGB colors, and green for redder colors (see main text for details). The RGBs in the stream's main part have similar average colors to the main galaxy's inner halo stars, with redder populations apparent on the outskirts of both the halo and stream. Panel (d) shows a star-count contour map of the stream, where the contour levels correspond to 5–10 stars per 50 arcsec^2 bin, in intervals of 1 star per bin.

stars.

5. STELLAR AND DYNAMICAL MASS

We now proceed to estimate the luminosities and masses of NGC 4449 and its stream. For NGC 4449, it is straightforward to add up the SDSS pixel fluxes inside the "optical radius" ($\mu_r = 25$ mag arcsec^{-2}). After correcting for extinction, we find $M_r = -17.8$. For the stream, we use the SDSS-calibrated BBRO image, integrating the flux within the faintest isophote that closes without including the main galaxy, which corresponds to $\mu_g = 26.75$ mag arcsec^{-2}. We find a stream magnitude of $M_r = -13.5$, which is comparable to the brightest Local Group dSphs, Fornax and And VII. Such galaxies have typical projected half-light radii of $\sim$ 0.4–1.0 kpc (Brodie et al. 2011), which is consistent with the stream's $\sim$ 0.8 kpc half-width.

For both galaxies, these luminosity estimates are lower-limits since they do not include potential extended low-surface-brightness features. In any case, the implied luminosity-ratio is $\sim$ 1:50.

To calculate stellar masses $M_\star$, we use two different approaches, adopting a Chabrier (2003) IMF (final mass, including remnants). The first is based on the integrated optical colors, following the relations between color and stellar mass-to-light-ratio ($\Upsilon_\star$) from Zibetti et al. (2009, Table B1). This paper also introduced a technique for mapping out pixel-by-pixel $\Upsilon_\star$ variations, which for NGC 4449 yields a total $M_\star = 7.46 \times 10^8 M_\odot$. For the stream, we assume a global color corresponding to the central SDSS measurement, $g - r = 0.45 \pm 0.1$. We then find a stream mass of $M_\star = 1.5^{+0.8}_{-0.6} \times 10^7 M_\odot$, implying a stellar mass-ratio between stream and host of $\sim$ 1:50, for any uniform IMF.

The second mass-estimation approach is to use the CMD, comparing observed star counts to predicted numbers from a stellar populations model. For the stream, we use the I-band stellar luminosity function near the TRGB, and normalize it to Monte Carlo simulations drawn assuming Z =0.001–0.004, and ages 2–10 Gyr. We obtain $M_\star \sim$ (2–5.5)$\times 10^7 M_\odot$ for the stream, which agrees with the color-based results. For the main galaxy, a similar approach was followed by McQuinn et al. (2010), whose results imply $M_\star = (1.2 \pm 0.2) \times 10^9 M_\odot$. This mass is somewhat higher than by using colors, but the CMD-based stellar-mass-ratio comes out to be similar, $\sim$ 1:40.

Remarkably, the mass of NGC 4449's stellar halo is similar to the stream's mass: based on the RGB counts of Ryś et al. (2011) and their normalization to K-band surface-brightness photometry, we estimate $M_\star \sim 2 \times 10^7 M_\odot$ for the halo between projected radii of 5–10 kpc. This halo could have therefore been built up directly by one or a few past accretion events similar to the present-day stream.

We next consider the dynamical masses of the host galaxy and its stream, including DM. The quantity that is arguably the most relevant to the current stream-galaxy interaction is the dynamical mass-ratio within the interaction region: the $\sim$ 14 kpc galactocentric radius. Based on the HI gas kinematics, we estimate an inclination-corrected circular velocity of $v_c \simeq 62$ km s^{-1} at this radius (Bajaja et al. 1994; Hunter et al. 2002), which means a dynamical mass for the main galaxy of $M_{\rm dyn}(r < 15$ kpc$) \simeq 1.1 \times 10^{10} M_\odot$. The HI gas mass is $\sim 10^9 M_\odot$ (Hunter et al. 1998), so this region is DM-dominated. Note that the v_c and $M_\star$ values together suggest that NGC 4449 is intermediate in mass to the LMC and SMC (cf. Besla et al. 2010).

For the stream mass, we turn to a plausibility argument based on Local Group dSphs, where the bright-

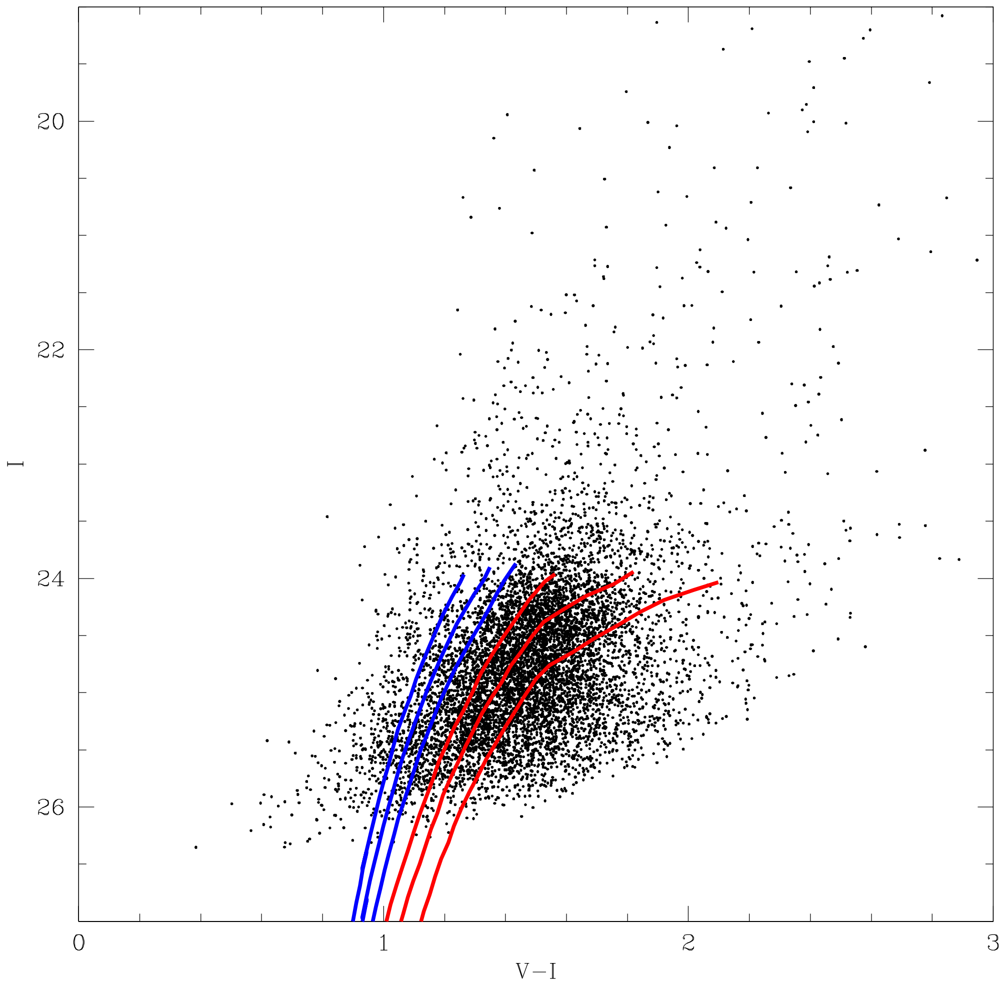

FIG. 3.— Color-magnitude diagram of the stream region, using Suprime-Cam $r'i'$ photometry transformed to Johnson-Cousins VI bands. RGB isochrones are overlaid from Girardi et al. (2002) for metallicities $Z = 0.001$ (blue curves) and $Z = 0.004$ (red curves). For each Z, the isochrones show ages of 2, 4, and 10 Gyr, from left to right, respectively.

est cases have estimated circular velocities of $v_c \sim$ 15–20 km s^{-1} on $\sim$ 1–3 kpc scales (Walker & Peñarrubia 2011; Boylan-Kolchin et al. 2011). Then if we assume the v_c values for both stream and main galaxy are fairly constant with radius, the ratio of v_c^2 yields the dynamical mass-ratio. This ratio is $\sim$ 1:20–1:10, and thus the stream may be significantly perturbing the main galaxy.

A final metric is the ratio of total (virial) halo masses $M_{\rm vir}$, which are not directly measurable but may be inferred on a statistical basis, assuming a ΛCDM framework. In this context, it is well-established that the total mass-to-light-ratios of dwarf galaxies increase dramatically at lower luminosities. Current estimates of $M_\star$-$M_{\rm vir}$ and luminosity-$M_{\rm vir}$ relations (Moster et al. 2010; Tollerud et al. 2011) would imply $M_{\rm vir} \sim (1\text{–}5)\times10^{11} M_\odot$ for NGC 4449, and $\sim (1\text{–}10)\times10^{10} M_\odot$ for the stream progenitor—for a plausible virial mass-ratio of $\sim$ 1:10–1:5.

Thus what appears to be a very minor merger in visible light may actually be closer to a *major* merger when including DM.

6. DISCUSSION

We have detected and analyzed a stellar tidal stream in the halo of NGC 4449 which we interpret as the ongoing disruption of a dSph galaxy by a larger dwarf (an LMC/SMC analogue). As far as we are aware, this is the lowest-mass primary galaxy with a verified stellar tidal stream.

We suggest some implications for galaxy evolution. It has been proposed that dSph's orbiting massive galaxies such as the Milky Way were "pre-processed" from gas-rich dwarfs by tidal effects within dwarf galaxy groups (D'Onghia et al. 2009). We may be witnessing such a transformation in action, with the HI streams surrounding NGC 4449 representing additional tidal debris.

We also suspect it is not just a coincidence that such a novel stream was found first around one of the most intensely star-forming nearby galaxies. The accretion event may well be the starburst trigger. The period of elevated star formation appears to have started around 0.5 Gyr ago (McQuinn et al. 2010), which is suggestively similar to the stream's $\sim$ 1–2 Gyr orbital period stream[16] (and more generally to any process that is linked to the

[16] Given a projected apocentric radius of $R_{\rm a}$ = 13 kpc,

dynamical time on $\sim$ 30 kpc scales).

One would now like to know how frequent such accretion events are among other dwarf galaxies in recent epochs. We suspect that exact analogues to this stream are not very common, or they would have been noticed already in DSS/SDSS images. However, if the stream had been only a bit fainter, more diffuse, or at a larger radius, it could have been missed, and thus there may be many more dwarf-hosted stellar streams awaiting detection.

In theory, the history of DM halo assembly should be fairly scale-free, and $\sim$ 1:10 mergers are expected to be the most generally dominant contributors to mass growth (Stewart et al. 2008). It is also increasingly recognized that such relatively minor mergers can have important effects on the larger galaxies, such as inciting global disk instabilities (Purcell et al. 2011).

If streams as in NGC 4449 are common in dwarfs, they re-ignite classic ideas about galaxy interactions triggering starbursts. Given the high rates of star formation in dwarf galaxies, it is natural to ask if satellites are responsible. Surveys along these lines have produced mixed results (Noeske et al. 2001; Brosch et al. 2004; Li et al. 2008), but until now, low-surface-brightness objects such as dSphs would have been missed.

Regardless of the implications for starbursts, dSph accretion appears to be an increasingly viable avenue for direct assembly of dwarf galaxies' stellar halos—as witnessed by NGC 4449, and by Fornax, which shows traces of swallowing an even smaller dSph (Coleman et al. 2005). Future observational determinations of dwarf stream frequency in combination with theoretical models may provide clues to the general substructure problem.

We thank Jay Strader for a preview of his paper and Monica Tosi for comments. Based on data collected at Subaru Telescope (operated by the National Astronomical Observatory of Japan), via Gemini Observatory time exchange (GN-2010B-C-204). FA received partial financial support from ASI, through contracts COFIS ASI-INAF I/016/07/0 and I/009/10/0. The Dark Cosmology Centre is funded by the Danish National Research Foundation. Work supported by the National Science Foundation (Grants AST-0808099, AST-0909237, AST-1109878, Graduate Research Fellowship), by NASA/Spitzer grant JPL-1310512, and by the UCSC-UARC Aligned Research Program.

a circular orbit provides a lower-limit for the period of $T = 2\pi R_a/v_c \simeq 1.3$ Gyr.

REFERENCES

Abazajian, K. N., Adelman-McCarthy, J. K., Agüeros, M. A., et al. 2009, ApJS, 182, 543

Annibali, F., Aloisi, A., Mack, J., Tosi, M., van der Marel, R. P., Angeretti, L., Leitherer, C., & Sirianni, M. 2008, AJ, 135, 1900 (A+08)

Annibali, F., Tosi, M., Aloisi, A., van der Marel, R. P., & Martinez-Delgado, D. 2011, ApJL, in press, arXiv:1111.5861

Arp, H. 1966, ApJS, 14, 1

Bajaja, E., Huchtmeier, W. K., & Klein, U. 1994, A&A, 285, 385

Besla, G., Kallivayalil, N., Hernquist, L., van der Marel, R. P., Cox, T. J., Keres, D. 2010, ApJ, 721, L97

Boylan-Kolchin, M., Bullock, J. S., & Kaplinghat, M. 2011, MNRAS, submitted, arXiv:1111.2048

Brodie, J. P., Romanowsky, A. J., Strader, J., & Forbes, D. A. 2011, AJ, 142, 199

Brosch, N., Almoznino, E., & Heller, A. B. 2004, MNRAS, 349, 357

Chabrier G., 2003, PASP, 115, 763

Cioni, M.-R. L., van der Marel, R. P., Loup, C. & Habing, H. J. 2000, A&A, 359, 601

Coleman, M. G., Da Costa, G. S., Bland-Hawthorn, J., & Freeman, K. C. 2005, AJ, 129, 1443

Cooper, A. P., Cole, S., Frenk, C. S., et al. 2010, MNRAS, 406, 744

D'Onghia, E., Besla, G., Cox, T. J., & Hernquist, L. 2009, Nature, 460, 605

Ferrero, I., Abadi, M. G., Navarro, J. F., Sales, L. V., & Gurovich, S. 2012, MNRAS, submitted, arXiv:1111.6609

Girardi, L., Bertelli, G., Bressan, A., Chiosi, C., Groenewegen, M. A. T., Marigo, P., Salasnich, B., & Weiss, A. 2002, A&A, 391, 195

Hartmann, L. W., Geller, M. J., & Huchra, J. P. 1986, AJ, 92, 1278

Huchtmeier, W. K., Karachentsev, I. D., & Karachentseva, V. E. 2009, A&A, 506, 677

Hunter, D. A., Wilcots, E. M., van Woerden, H., Gallagher, J. S., & Kohle, S. 1998, ApJ, 495, L47

Hunter, D. A., van Woerden, H., & Gallagher, J. S. 1999, AJ, 118, 2184

Hunter, D. A., Rubin, V. C., Swaters, R. A., Sparke, L. S., & Levine, S. E. 2002, ApJ, 580, 194

Karachentsev, I. D., Karachentseva, V. E., & Huchtmeier, W. K. 2007, Astronomy Letters, 33, 512

Li, C., Kauffmann, G., Heckman, T. M., Jing, Y. P., & White, S. D. M. 2008, MNRAS, 385, 1903

Lovell, M., Eke, V., Frenk, C., et al. 2011, MNRAS, submitted, arXiv:1104.2929

Marigo, P., Girardi, L., & Chiosi, C. 2003, 403, 225

Martínez-Delgado, D., Alonso-García, J., Aparicio, A., & Gómez-Flechoso, M. A. 2001, ApJ, 549, L63

Martínez-Delgado, D., Peñarrubia, J., Gabany, R.J., Trujillo, I., Majewski, S.R., & Pohlen, M. 2008, ApJ, 689, 184

Martínez-Delgado, D., Pohlen, M., Gabany, R. J., et al. 2009, ApJ, 692, 955

Martínez-Delgado, D., Gabany, R. J., Crawford, K., et al. 2010, AJ, 140, 962

McConnachie, A. W., Irwin, M. J., Ibata, R. A., et al. 2009, Nature, 461, 66

McQuinn, K. B. W., et al. 2010, ApJ, 724, 49

Miyazaki, S., et al. 2002, PASJ, 54, 833

Mo, H., van den Bosch, F. C., & White, S. 2010, Galaxy Formation and Evolution. Cambridge University Press, 2010. ISBN: 9780521857932,

Moster, B. P., Somerville, R. S., Maulbetsch, C., et al. 2010, ApJ, 710, 903

Noeske, K. G., Iglesias-Páramo, J., Vílchez, J. M., Papaderos, P., & Fricke, K. J. 2001, A&A, 371, 806

Ouchi, M., et al. 2004, ApJ, 611, 660

Purcell, C. W., Bullock, J. S., & Zentner, A. R. 2007, ApJ, 666, 20

Purcell, C. W., Bullock, J. S., Tollerud, E. J., Rocha, M., & Chakrabarti, S. 2011, Nature, 477, 301

Ryś, A., Grocholski, A. J., van der Marel, R. P., Aloisi, A., & Annibali, F. 2011, A&A, 530, A23

Schweizer, F., & Seitzer, P. 1988, ApJ, 328, 88

Schlegel, D. J., Finkbeiner, D. P., & Davis, M. 1998, ApJ, 500, 525

Stetson, P. B. 1987, PASP, 99, 191

Stewart, K. R., Bullock, J. S., Wechsler, R. H., Maller, A. H., & Zentner, A. R. 2008, ApJ, 683, 597

Stinson, G. S., Dalcanton, J. J., Quinn, T., et al. 2009, MNRAS, 395, 1455

Strader, J., Seth, A. C., & Caldwell, N. 2011, submitted

Tollerud, E. J., Bullock, J. S., Graves, G. J., & Wolf, J. 2011, ApJ, 726, 108

Tolstoy, E., Hill, V., & Tosi, M. 2009, ARA&A, 47, 371

Walker, M. G., & Peñarrubia, J. 2011, ApJ, 742, 20

Weisz, D. R., Dalcanton, J. J., Williams, B. F., et al. 2011, ApJ, 739, 5

Zibetti S., Charlot S., Rix H., 2009, MNRAS, 400, 1181